

W and Z/γ^* boson production in association with a bottom-antibottom pair

Rikkert Frederix

*Institut für Theoretische Physik, Universität Zürich, Winterthurerstrasse 190,
CH-8057 Zürich, Switzerland*

KITP, University of California Santa Barbara, CA 93106-4030, USA

Stefano Frixione*

PH Department, TH Unit, CERN, CH-1211 Geneva 23, Switzerland

ITPP, EPFL, CH-1015 Lausanne, Switzerland

Valentin Hirschi

ITPP, EPFL, CH-1015 Lausanne, Switzerland

Fabio Maltoni

Centre for Cosmology, Particle Physics and Phenomenology (CP3)

Université catholique de Louvain, B-1348 Louvain-la-Neuve, Belgium

Roberto Pittau

Departamento de Física Teórica y del Cosmos y CAFPE, Universidad de Granada

PH Department, TH Unit, CERN, CH-1211 Geneva 23, Switzerland

KITP, University of California Santa Barbara, CA 93106-4030, USA

Paolo Torrielli

ITPP, EPFL, CH-1015 Lausanne, Switzerland

ABSTRACT: We present a study of $\ell\nu b\bar{b}$ and $\ell^+\ell^-b\bar{b}$ production at hadron colliders. Our results, accurate to the next-to-leading order in QCD, are based on automatic matrix-element calculations performed by MADLOOP and MADFKS, and are given at both the parton level, and after the matching with the HERWIG event generator, achieved with aMC@NLO. We retain the complete dependence on the bottom-quark mass, and include exactly all spin correlations of final-state leptons. We discuss the cases of several observables at the LHC which highlight the importance of accurate simulations.

KEYWORDS: LHC, NLO, Monte Carlo.

*On leave of absence from INFN, Sezione di Genova, Italy.

Contents

| | |
|-----------------------------------|-----------|
| 1. Introduction | 1 |
| 2. Results | 3 |
| 3. Conclusions and outlook | 14 |
| 4. Acknowledgments | 15 |

1. Introduction

The discovery and identification of new degrees of freedom and interactions at high-energy colliders relies on the detailed understanding of Standard Model (SM) background processes. Prominent among these is the production of electroweak bosons (W, Z) in association with jets, of which one or more possibly contain bottom quarks. The prime example is the observation of the top quark at the Fermilab Tevatron collider, produced either in pairs [1, 2] or singly [3, 4], since both of these mechanisms typically lead to W plus b -jets signatures. Other crucial examples involve the search for a SM Higgs in association with vector bosons (WH/ZH), with the subsequent Higgs decay into a $b\bar{b}$ pair, a sought-for discovery channel both at the Tevatron [5] and at the LHC [6, 7]. Finally, in models which feature an extended Higgs sector, such as the MSSM or more generally a two-Higgs doublet model, a typical Higgs discovery channel is through $Hb\bar{b}$ and $Ab\bar{b}$ final states, with an $H/A \rightarrow \tau^+\tau^-$ decay. In this case, the SM process $\ell^+\ell^-b\bar{b}$ can provide an important reference measurement.

Next-to-leading-order (NLO) QCD calculations for the production of a vector boson in association with jets have by now quite a successful record. Accurate predictions for W plus up to four light jets [8, 9, 10, 11, 12, 13] and for Z plus up to three light jets [14, 8, 9, 15] have become available in the past few years. Associated production with heavy quarks, and in particular with bottom quarks, has been studied using various approximations. The $Wb\bar{b}$ and $Zb\bar{b}$ processes have been calculated at the NLO for the first time in refs. [16] and [17] respectively, by setting the bottom-quark mass equal to zero. Such calculations can be used only for observables that contain at least two b -jets. The same processes have been considered again in refs. [18, 19, 20], where a non-zero bottom-quark mass has been used; however, the matrix elements still involved on-shell vector bosons, thereby neglecting spin correlations of the leptons emerging from W and Z decays. In the case of W production, this limitation has been recently lifted in ref. [21], which presents the NLO calculation for the leptonic process $\ell\nu b\bar{b}$. Other NLO calculations for final states with one b -jet, Wb and Zb [22, 23], and one b -jet plus a light jet, Wbj and Zbj [24, 25], are also

available in the five-flavour scheme. All such calculations have played a role and/or have been extensively compared to the data collected at the Tevatron [26, 27, 28, 29], and now start to be considered in LHC analyses as well [30, 31].

In this paper we present a calculation of $\ell\nu b\bar{b}$ production that includes NLO QCD corrections (analogous to that of ref. [21]), and the first calculation at the NLO of $\ell^+\ell^-b\bar{b}$ production with massive bottom quarks; we retain the full spin correlations of the final-state leptons¹. Furthermore, we match both of these results to the HERWIG event generator by adopting the MC@NLO formalism [32]. Therefore, our results include all the relevant features which are important in experimental analyses, and can be used in order to obtain NLO predictions for a large class of observables, including those with zero, one and two b -jets. All aspects of the calculations are fully automated and analogous to the calculation recently appeared for $Ht\bar{t}/At\bar{t}$ production [33]. One-loop amplitudes are evaluated with MADLOOP [34], whose core is the OPP integrand reduction method [35] as implemented in CUTTOOLS [36]. Real contributions and the corresponding phase-space subtractions, achieved by means of the FKS formalism [37], as well as their combination with the one-loop and Born results and their subsequent integration, are performed by MADFKS [38]. The MC@NLO matching is also fully automated, and allows us to simulate for the first time $\ell\nu b\bar{b}$ and $\ell^+\ell^-b\bar{b}$ production with NLO accuracy, including *exactly* spin correlations, off-shell and interference effects, and hadron-level final states. All the computations are integrated in a single software framework, which we have dubbed aMC@NLO in ref. [33]. We point out that the on-shell- W result of ref. [18] has recently been matched to showers in ref. [39] in the framework of the POWHEG box [40].

The phenomenology of $\ell\nu b\bar{b}$ and $\ell^+\ell^-b\bar{b}$ final states is very rich and in fact transcends the prosaic role of background for Higgs or top-quark physics. Thanks to the aMC@NLO implementation, several QCD issues interesting on their own can now be addressed theoretically and the results efficiently compared to experiments. In this work we limit ourselves to providing new evidence that reliable and flexible predictions for the $\ell\nu b\bar{b}$ and $\ell^+\ell^-b\bar{b}$ processes need to include:

- NLO corrections;
- bottom quark mass effects;
- spin-correlation and off-shell effects;
- showering and hadronisation.

Detailed studies of these processes as backgrounds to specific signals, such as single-top and $Hb\bar{b}$ or $Ab\bar{b}$ production respectively, are left to forthcoming investigations.

This paper is organised as follows. In the next section we present several distributions relevant to $\ell\nu b\bar{b}$ and $\ell^+\ell^-b\bar{b}$ production at the LHC, and report the results for total rates at both the Tevatron and the LHC. By working with a non-zero bottom mass, we are able

¹In the rest of this paper, $\ell\nu b\bar{b}$ and $\ell^+\ell^-b\bar{b}$ production as predicted by our simulations may also be denoted by $Wb\bar{b}$ and $Zb\bar{b}$ respectively.

to obtain predictions for the cases in which one or two b 's are not observed, and can thus have arbitrarily small transverse momenta. We also give one example of the comparisons, at the level of hadronic final states, between the HW and HZ signals and their respective irreducible backgrounds which we have computed in this paper. We draw our conclusions in sect. 3.

2. Results

At the leading order (LO) in QCD $\ell\nu b\bar{b}$ and $\ell^+\ell^-b\bar{b}$ production at hadron colliders proceed through different channels. Both final states can be obtained via a Drell-Yan-type mechanism, i.e., $q\bar{q}^{(\prime)}$ annihilation in association with a gluon splitting in a $b\bar{b}$ pair, see fig. 1(a). $Zb\bar{b}$, however, can also be produced by gluon fusion, see fig. 1(b), a channel that at the LO contributes a 30% of the total rate at the Tevatron, but turns out to be the dominant one (80%) at the LHC, owing to the larger gluon luminosity there. As we shall see in the following, the fact that $Wb\bar{b}$ and $Zb\bar{b}$ production are dominated by different channels at the LHC leads to important differences in the kinematical properties of final states, and in particular of b -jets.

We start by presenting results for the total cross sections at both the Tevatron, $\sqrt{s} = 1.96$ TeV, and the LHC, $\sqrt{s} = 7$ TeV; the $\ell\nu b\bar{b}$ results are the sums of the $\ell^+\nu b\bar{b}$ and $\ell^-\bar{\nu} b\bar{b}$ ones (due to virtual- W^+ and W^- production respectively). In our computations we have set the lepton masses equal to zero, and is therefore not necessary to specify their flavour, which we generically denote by ℓ (for the charged leptons) and ν (for the neutrinos); we always quote results for one flavour. For the numerical analysis we have chosen:

$$\mu_F^2 = \mu_R^2 = m_{\ell\nu}^2 + p_T^2(\ell\ell') + \frac{m_b^2 + p_T^2(b)}{2} + \frac{m_{\bar{b}}^2 + p_T^2(\bar{b})}{2}, \quad (2.1)$$

with $\ell\ell' = \ell\nu$ and $\ell\ell' = \ell^+\ell^-$ in the case of $Wb\bar{b}$ and $Zb\bar{b}$ production respectively; the value of the b -quark mass is that of the pole mass, $m_b = 4.5$ GeV. We have used LO and NLO MSTW2008 four-flavour parton distribution functions [41] for the corresponding cross sections, and the SM-parameter settings can be found in table 1. Given that the primary aim of this paper is not that of presenting precise comparisons with data, but rather

| Parameter | value | Parameter | value |
|----------------------------------|----------|---------------|-------------------------|
| m_Z | 91.118 | α^{-1} | 132.50698 |
| m_W | 80.419 | G_F | $1.16639 \cdot 10^{-5}$ |
| m_b | 4.5 | CKM $_{ij}$ | δ_{ij} |
| m_t | 172.5 | Γ_Z | 2.4414 |
| $\alpha_s^{(\text{LO},4)}(m_Z)$ | 0.133551 | Γ_W | 2.0476 |
| $\alpha_s^{(\text{NLO},4)}(m_Z)$ | 0.114904 | | |

Table 1: Settings of physical parameters used in this work, with dimensionful quantities given in GeV.

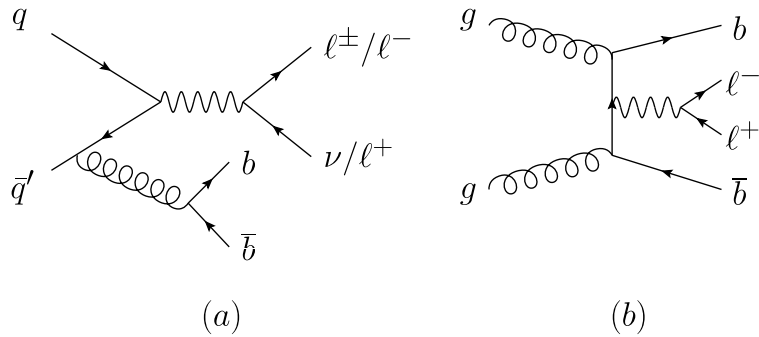


Figure 1: Representative diagrams contributing to $\ell\nu b\bar{b}$ and $\ell^+\ell^-b\bar{b}$ production at the leading order. $\ell\nu b\bar{b}$ production can proceed only via a $q\bar{q}'$ channel, diagram (a). For $\ell^+\ell^-b\bar{b}$ production the $q\bar{q}$ channel, diagram (a), is dominant at the Tevatron, while the gg channel, diagram (b), largely dominates at the LHC.

| | Cross section (pb) | | | | | |
|------------------------|--------------------------------|-------|------------|------------------------|------|------------|
| | Tevatron $\sqrt{s} = 1.96$ TeV | | | LHC $\sqrt{s} = 7$ TeV | | |
| | LO | NLO | K factor | LO | NLO | K factor |
| $\ell\nu b\bar{b}$ | 4.63 | 8.04 | 1.74 | 19.4 | 38.9 | 2.01 |
| $\ell^+\ell^-b\bar{b}$ | 0.860 | 1.509 | 1.75 | 9.66 | 16.1 | 1.67 |

Table 2: Total cross sections for $\ell\nu b\bar{b}$ and $\ell^+\ell^-b\bar{b}$ production at the Tevatron ($p\bar{p}$ collisions at $\sqrt{s} = 1.96$ TeV) and the LHC (pp collisions at $\sqrt{s} = 7$ TeV), to LO and NLO accuracy. These rates are relevant to one lepton flavour, and the results for $\ell\nu b\bar{b}$ production are the sums of those for $\ell^+\nu b\bar{b}$ and $\ell^-\bar{\nu} b\bar{b}$ production. The integration uncertainty is always well below 1%.

that of studying the defining features of the production mechanisms, in the CKM matrix (relevant to the $Wb\bar{b}$ results) we have neglected off-diagonal terms: this cannot change the conclusions we shall arrive at, but helps reduce the computing time. It should be clear that this is not a limitation of the code, since a non-diagonal CKM matrix can simply be given in input if one so wishes. Our runs are fully inclusive and no cuts are applied at the generation level, except for $m_{\ell^+\ell^-} > 30$ GeV in the $\ell^+\ell^-b\bar{b}$ sample. The predicted production rates at the Tevatron and at the LHC are given in table 2 where, for ease of reading, we also show the fully inclusive K factors. The contribution of the $gg \rightarrow Zb\bar{b} + X$ channels is clearly visible in these results: at the Tevatron $\sigma(\ell^+\ell^-b\bar{b})/\sigma(\ell\nu b\bar{b})$ is quite small (and of the same order of the ratio of the fully-inclusive cross sections $\sigma(Z)/\sigma(W)$), whereas at the LHC $\ell^+\ell^-b\bar{b}$ and $\ell\nu b\bar{b}$ differ only by a factor of two.

We now study the impact of NLO QCD corrections on differential distributions, at both the parton level and after showering and hadronisation, and in doing so we limit ourselves to the case of the LHC, where the kinematical differences between $Wb\bar{b}$ and $Zb\bar{b}$ production are more evident. The parton shower in aMC@NLO has been performed with

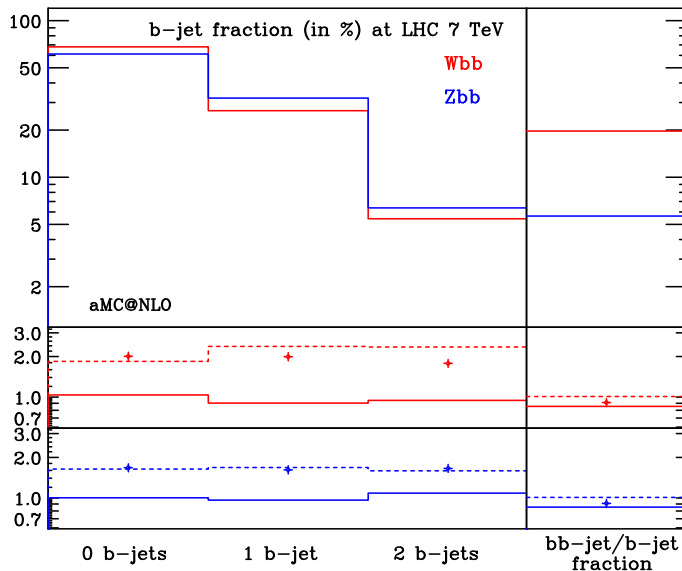


Figure 2: Fractions of events (in percent) that contain: zero b -jets, exactly one b -jet, and exactly two b -jets. The rightmost bin displays the fraction of b -jets which are bb -jets. The two insets show the ratio of the aMC@NLO results over the corresponding NLO (solid), aMC@LO (dashed), and LO (symbols) ones, separately for $Wb\bar{b}$ (upper inset) and $Zb\bar{b}$ (lower inset) production.

fortran HERWIG [42, 43, 44], version 6.520².

We start by summarizing our results for b -jet rates. Jets are reconstructed at the particle level. In the case of MC simulations, this means giving all final-state stable hadrons³ in input to the jet algorithm. We adopt the anti- k_T jet clustering algorithm [49] with $R = 0.5$, and require each jet to have $p_T(j) > 20$ GeV and $|\eta(j)| < 2.5$. A b -jet is then defined as a jet that contains *at least* one b -hadron; a bb -jet is a jet that contains at least two b -hadrons (hence, a bb -jet is also a b -jet). This implies that we make no distinction between the b quark and antiquark contents of a jet. We point out that at least another definition of b -jets exists [50] which has a better behaviour in the $m_b \rightarrow 0$ limit, in the sense that it gives (IR-safe) results consistent with the naive picture of “quark” and “gluon” jets. In practice, this is relevant only in the $p_T \gg m_b$ limit. Since this region is not our primary interest in this paper, we stick to the usual definition; however, it should be obvious that any jet definition can be used in our framework.

In fig. 2 we present b -jet rates, as the fractions of events that contain zero, exactly one, or exactly two b -jet(s). In the case of MC-based simulations, there are also events with more than two b -jets and more than one bb -jet, but they give a relative contribution to the total rate equal to about 0.4% (for $Wb\bar{b}$) and 0.6% (for $Zb\bar{b}$), and are therefore not reported here. The rightmost bin of fig. 2 shows the fraction of b -jets which are bb -jets. There is an inset for each of the two histograms shown in the upper part of fig. 2. Each of the insets presents three curves, obtained by computing the ratio of the aMC@NLO

²Automation of the matching to parton shower in the MC@NLO formalism to HERWIG++ [45] and to PYTHIA [46] (see refs. [47] and [48] respectively) is currently under way.

³In order to simplify the HERWIG analyses, weakly-decaying B hadrons are set stable.

results over the NLO (solid), aMC@LO⁴ (dashed), and LO (symbols) corresponding ones. The b -jet fractions are fairly similar for $Wb\bar{b}$ and $Zb\bar{b}$ production, and the effects of the NLO corrections are consistent with the fully-inclusive K factors. On the other hand, the bb -jet contribution to the b -jet rate is seen to be more than three times larger for $\ell\nu b\bar{b}$ than for $\ell^+\ell^-b\bar{b}$ final states. This fact is again related to the different mechanisms for the production of a $b\bar{b}$ pair in the two processes considered here. At variance with the case of $\ell\nu b\bar{b}$ production, in a $\ell^+\ell^-b\bar{b}$ final state the two b 's may come from the separate branchings of two initial-state gluons, and thus the probability of them ending in the same jet is much smaller than in the case of a $g \rightarrow b\bar{b}$ final-state branching. We conclude this discussion by pointing out that the zero- and one- b -jet rates can only be obtained with a non-zero b -quark mass, since the one or two “untagged” b 's must be integrated down to $p_T = 0$, and hence $m_b \neq 0$ is required in order to screen initial-state collinear divergences. This fact is a severe test condition for the computer programs used in the computations, because it may induce numerical instabilities. We stress that we did not impose low- p_T cuts on any of the final-state particles in MADLOOP, MADFKS, and in the generation of hard events in aMC@NLO; our results are therefore completely unbiased, which is what gives us the possibility of computing quantities such as those reported in table 2 and in fig. 2.

We now turn to studying differential distributions, and start by considering those defined in terms of final-state leptons. Observables sensitive to the hadronic activity of the events, be either relevant to b -jets or to B -hadrons, will follow later. In the case of MC-based simulations, several leptons can appear in the final state. We use the MC-truth information to select the two which emerge from the hard process, and we shall simply refer to them as “the leptons” henceforth. A more realistic analysis may select leptons on the basis of their hardness, measured e.g. with their p_T 's; in practice, for the processes we are considering here (and thanks to the fact that the b -hadrons have been set stable) the two approaches are equivalent.

In fig. 3 the invariant mass of the final-state lepton pairs is shown. The effect of the γ^* contribution to $\ell^+\ell^-b\bar{b}$ production is clearly visible at small invariant masses. In this plot, with limit ourselves to presenting only the aMC@NLO results, since the other simulations give results which are essentially identical to the present ones.

In figs. 4 and 5 the transverse momenta and the pseudorapidities of the charged leptons are shown separately according to their electric charges. In the two upper insets we have used the same patterns and conventions as in fig. 2 – these will be used throughout this paper. In the case of $Wb\bar{b}$ production, the effects of the NLO corrections are especially pronounced at large p_T 's, where they are the signal of new partonic subprocesses opening up at this order, and in particular of those which include an initial-state gluon, such as gg . Results after matching with showers consistently show a similar behaviour. The same large enhancement is not present in the case of Z production, which receives gluon-initiated contributions already at the LO; again, this trend is seen also after matching with showers. The lowest insets (solid magenta curves) show the ratios of the aMC@NLO results relevant

⁴We call aMC@LO the analogue of aMC@NLO, in which the short-distance cross sections are computed at the LO rather than at the NLO. Its results are therefore equivalent to those one would obtain by using, e.g., MADGRAPH/MADEVENT [51] interfaced to showers.

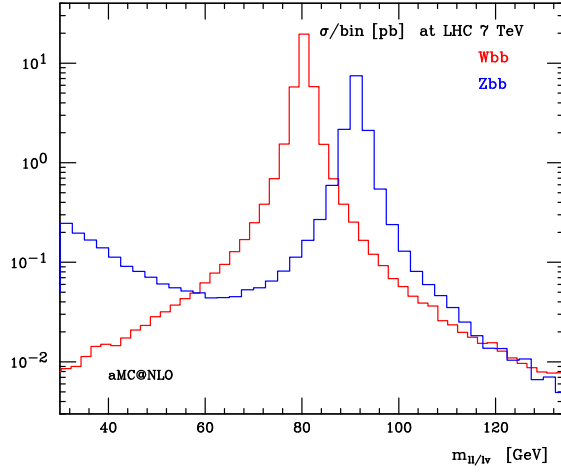


Figure 3: Invariant mass distribution of final-state lepton pairs, as predicted by aMC@NLO.

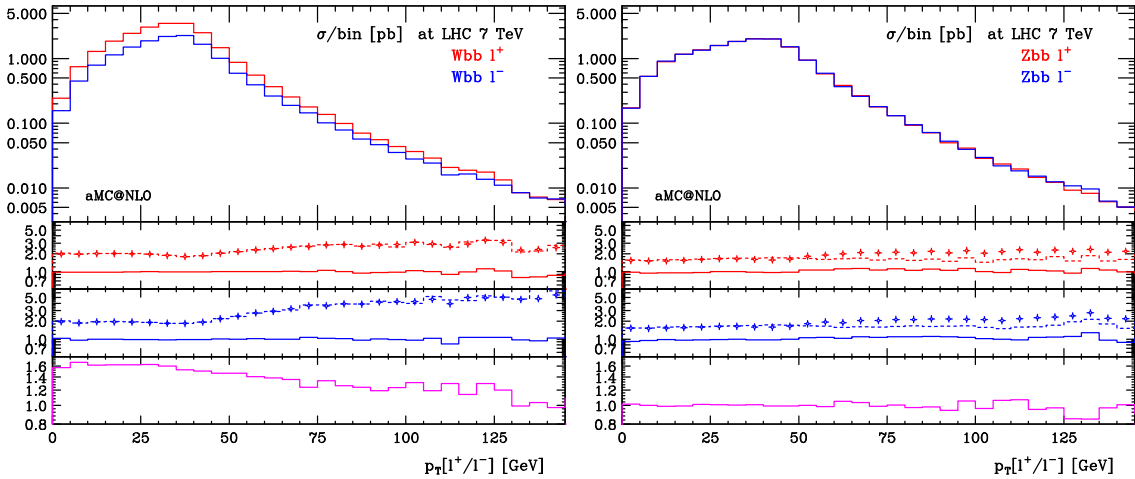


Figure 4: Transverse momentum of the charged leptons in $l\nu b\bar{b}$ (left panel) and $l^+l^-b\bar{b}$ (right panel) production, shown separately for positive and negative charges. The upper and middle insets follow the same patterns as those in fig. 2. The lower inset (magenta solid histogram) is the ratio of the aMC@NLO results relevant to positively-charged leptons over those relevant to negatively-charged ones.

to positively-charged leptons over those relevant to negatively-charged ones. In the case of $Wb\bar{b}$ production the behaviour is similar to what has been described recently in ref. [52], while for $Zb\bar{b}$ this distribution is flat, as expected.

A complementary aspect of the different parton luminosities that contribute to $Wb\bar{b}$ and $Zb\bar{b}$ production can be appreciated by looking for example at the transverse momentum distributions of the $l\nu$ and l^+l^- pairs (i.e. of the virtual W and Z bosons respectively), shown in the left panel of fig. 6. In the case of $l\nu b\bar{b}$ final states, the aMC@LO and LO results are very close to each other, which is not the case for $l^+l^-b\bar{b}$ production. This is due to the fact that the gg -initiated channel in the latter case is responsible for much more QCD radiation in MC-based simulations than the $q\bar{q}$ channel (the latter being identical to

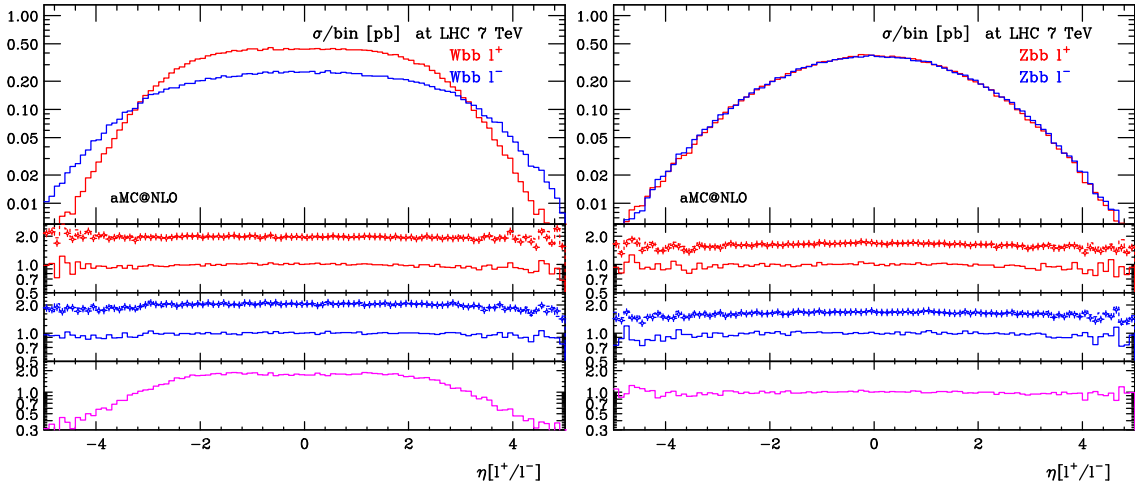


Figure 5: As in fig. 4, for the pseudorapidity of the charged leptons.

the mechanism that induces $Wb\bar{b}$ production). This larger amount of radiation hardens the virtual- Z p_T spectrum predicted by aMC@LO, making it more similar to the aMC@NLO result than in the case of $Wb\bar{b}$ production. The NLO p_T spectra of the virtual vector bosons are closer to the aMC@NLO results, because at that order one does get contributions from gluon-initiated channels to both $\ell\nu b\bar{b}$ and $\ell^+\ell^-b\bar{b}$ final states, and thus the relative changes obtained when matching with parton showers have a milder impact. This is an example of the “stabilizing” pattern that one observes when higher-order perturbative results are taken into account. On the other hand, the rapidity distributions of the lepton pairs do not change significantly under QCD radiation, as is shown in the right panel of fig. 6.

We remark that we do not find any significant enhancement in the large- p_T tails of vector bosons when going from the NLO to the aMC@NLO predictions, at variance with the POWHEG $Wb\bar{b}$ result of ref. [39] which necessitates an ad-hoc *perturbative* tuning for this reason. It should further be stressed that the almost perfect coincidence between the aMC@LO and LO results for $p_T(\ell\nu)$ may not occur by simply changing the tuning of the shower parameters in HERWIG: indeed, we have verified that the spectrum predicted by PYTHIA 6 is slightly different w.r.t. the aMC@LO or LO ones. It is also interesting to notice that the features discussed here and that affect the low- and intermediate- p_T regions of lepton pairs are not visible in the case of the individual lepton p_T spectra, fig. 4. We have verified that kinematical correlations are such that, for a fixed small or intermediate value of $p_T(\ell^\pm)$, one integrates over a $p_T(\ell^+\ell^-)$ range that causes the local differences between the aMC@LO and LO results for the latter transverse momentum to be averaged out.

The left panel of fig. 7 presents the $\cos\theta^*$ distribution, computed by separating the positively- and negatively-charged lepton contributions. We remind the reader that such an observable is defined as the cosine of the angle between the chosen charged lepton, and the direction of flight of the parent vector boson, in the rest frame of the latter. Clearly visible are the strong angular correlations and charge asymmetry in the $\ell\nu b\bar{b}$ case. For $\ell^+\ell^-b\bar{b}$ production such correlations and asymmetries, while present, are much milder, and

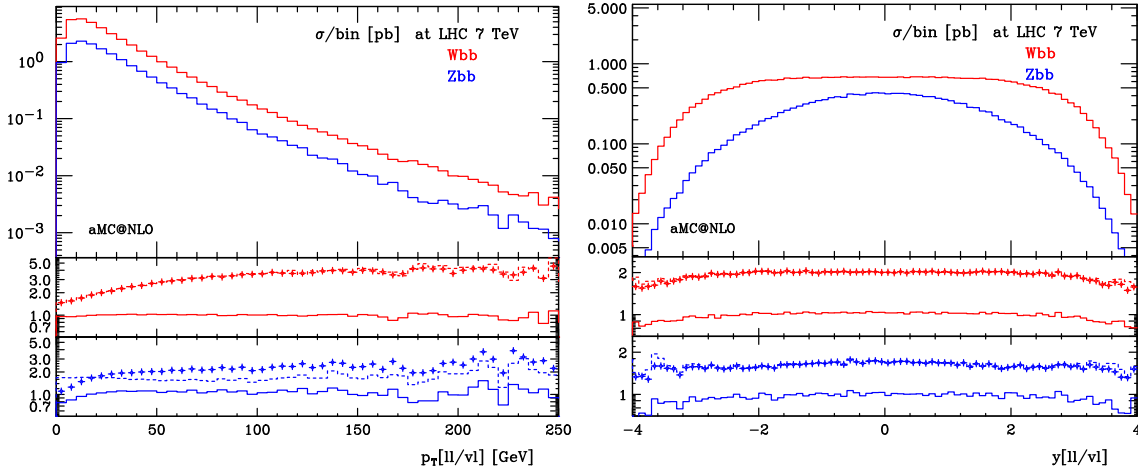


Figure 6: Transverse momentum (left panel) and rapidity (right panel) of the $\ell\nu$ and $\ell^+\ell^-$ pairs (i.e. of the virtual W and Z bosons respectively) in $\ell\nu b\bar{b}$ and $\ell^+\ell^- b\bar{b}$ production. The insets follow the same patterns as those in fig. 2.

likely not observable in a real experiment. For both processes, the aMC@NLO results are basically identical to those of aMC@LO, NLO, and LO, and thus we refrain from showing the latter here.

In the right panel of fig. 7, where we consider only leptons with positive electric charge to be definite, we plot the ratio of the lepton transverse momentum over the same quantity, obtained by imposing a phase-space (i.e., flat) decay of the parent vector boson; hence, this ratio is a measure of the impact of spin correlations on the inclusive-lepton p_T . We see that differences between correlated and uncorrelated decays can be as large as 20%, and vary across the kinematical range considered. This confirms that the inclusion of spin-correlation effects is necessary when an accurate description of the production process is required. We stress again that our computations feature spin correlations exactly at the matrix-element level, including one-loop ones. It is interesting to observe that, while in the case of $Zb\bar{b}$ production all four calculations give similar results (see the lower inset), this happens in $Wb\bar{b}$ production only for $p_T(\ell^+) \lesssim 50$ GeV (see the upper inset). At p_T values larger than this, aMC@NLO and NLO predict ratios that differ from the corresponding aMC@LO and LO ones. Once again, this is a manifestation of the significant impact of gluon-initiated, NLO partonic processes on $Wb\bar{b}$ cross sections, and is consistent with the findings of ref. [52] (relevant to the associated production of W bosons with light jets).

In figs. 8 and 9 the transverse momenta and the pseudorapidities of the two hardest b -jets are shown. Differences in normalisation are consistent with what we expect on the basis of inclusive K factors; differences in shapes are typically small, but visible. We point out that for an event to contribute to the hardest- b -jet observables shown here it is sufficient that one b -jet be present in the event; the other b quark emerging from the hard process can have arbitrarily small momentum.

In the left panel of fig. 10, the ΔR separation between the two hardest b -hadrons (for the MC-based simulations) or between the b and \bar{b} quarks (for the NLO and LO

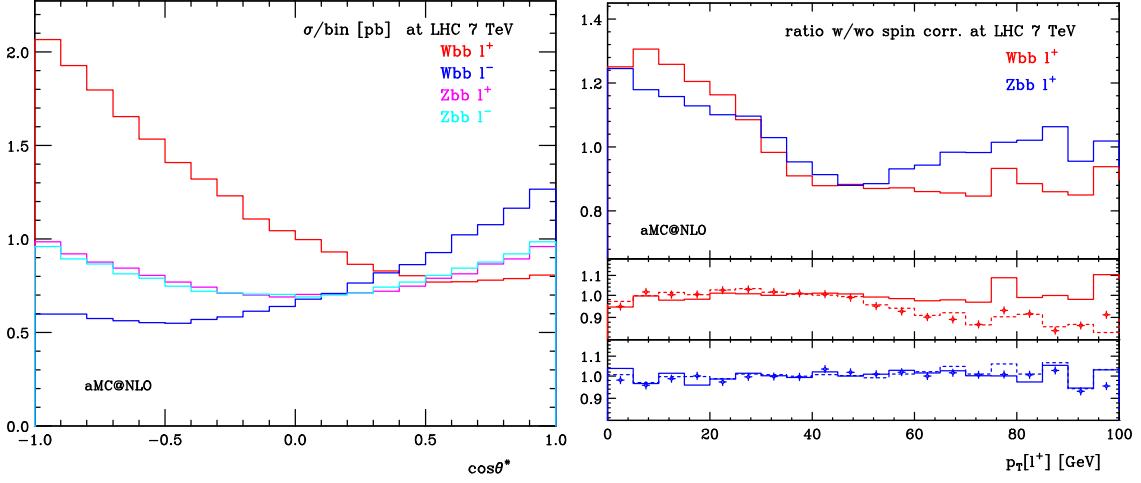


Figure 7: Left panel: $\cos\theta^*$ distribution of final-state charged leptons for different charges. All histograms have been obtained with aMC@NLO. See the text for the observable definition. Right panel: ratio of the results for the p_T of the positively-charged lepton over the same quantity computed by neglecting production spin correlations. The insets follow the same patterns as those in fig. 2.

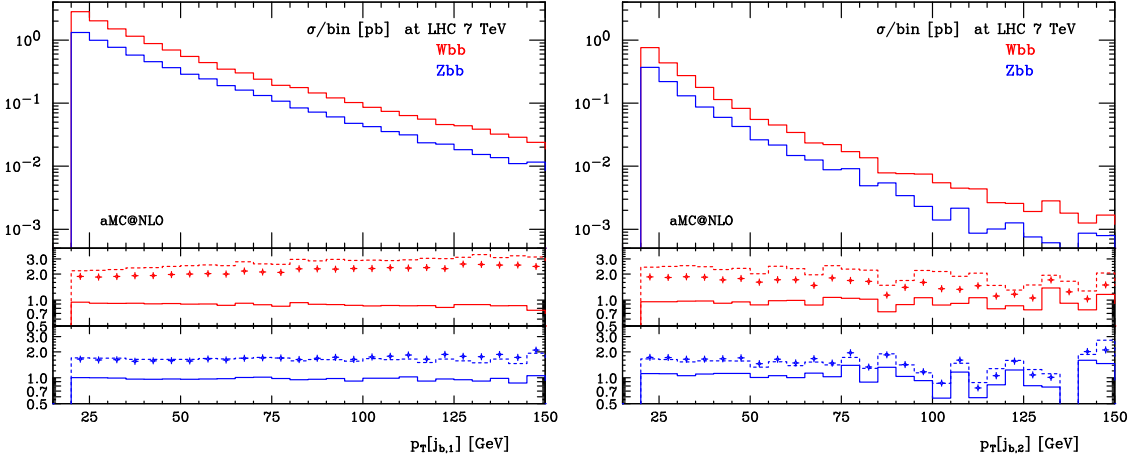


Figure 8: Transverse momentum of the hardest (left panel) and second-hardest b -jet (right panel) in $Wb\bar{b}$ and $Zb\bar{b}$ production. The insets follow the same patterns as those in fig. 2.

computations) is shown. Differences between the $Wb\bar{b}$ and $Zb\bar{b}$ processes are manifest. In the former case the two b 's originate from a final-state gluon splitting, and they will thus tend to be quite close in pseudorapidity. On the other hand, the two b 's in $Zb\bar{b}$ production can arise from the uncorrelated branchings of the initial-state gluons in the gg channel, and in this way they will naturally acquire a large separation in pseudorapidity, which is directly related with large- ΔR values. However, a $b\bar{b}$ pair arising from a final-state gluon branching can be easily separated in pseudorapidity by QCD radiation. This is the reason why the parton-level LO result in the case of $Wb\bar{b}$ production is so different from the other three predictions (as shown by the symbols in the upper inset). Both parton-level NLO (through

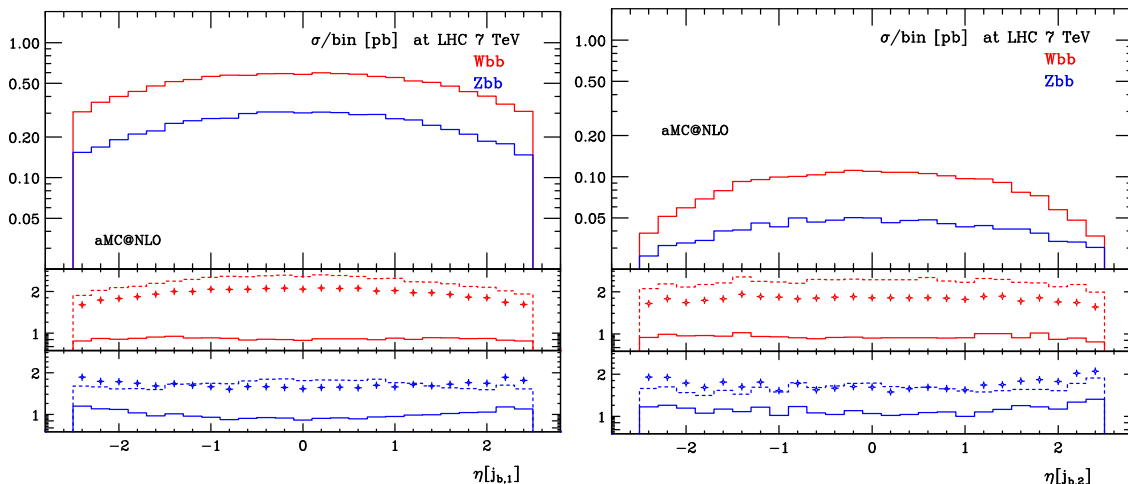


Figure 9: As in fig. 8, for the pseudorapidity of the hardest and the second-hardest b -jet.

radiation present at the matrix-element level) and aMC@LO (through radiation due to parton showers) results are in fact much closer to aMC@NLO than parton-level LO result is. This does not happen in the case of $Zb\bar{b}$ production, since as discussed before the b and \bar{b} quarks can be well-separated in pseudorapidity already at the LO. It should be stressed that the b -hadrons that contribute to the ΔR separation shown in fig. 10 are not subject to any lower cuts in p_T . Thus, one expects that the effects of extra radiation be diminished when imposing a p_T cut or, which is equivalent, by studying the same distribution in the case of b -jets. We have verified that this is indeed the case, i.e. that when a minimum- p_T cut is imposed on the two b -hadrons the pattern of NLO QCD corrections in $Wb\bar{b}$ production is more similar to that observed in $Zb\bar{b}$ production. This is another example of the possibility of testing detailed properties of QCD radiation by considering low- p_T events. It should be clear that from the theoretical viewpoint such studies can be sensibly performed only by retaining the full b -mass dependence.

The right panel of fig. 10 shows the mass of the b -jets in the events. The observable is inclusive over all b -jets, which implies that a given event may enter more than once in the plot. Striking is the onset of the bb -jet contribution in the $Wb\bar{b}$ result around $m_{j_b} \approx 12$ GeV. In the case of $Zb\bar{b}$ production this effect is almost invisible, a consequence of the fact that the fraction of events where a b -jet is actually a bb -jet is much smaller than for $Wb\bar{b}$ production, see fig. 2. The distribution discussed here measures the activity inside a jet, and one cannot expect fixed-order parton-level results, where a jet consists of one or two particles, to be particularly sensible in this case. In fact, we see that fixed-order results are very different from MC-based ones. On the other hand, the differences in shape when going from aMC@LO to aMC@NLO are small, in particular for $Zb\bar{b}$ production, as expected for observables which are insensitive to emissions at large relative p_T 's. We also point out that the knee at $m_{j_b} \approx 12$ GeV would appear as a feature of *gluon* jets if the b -jet definition of ref. [50] were used. This stresses again the fact that, at small and moderate p_T 's, the usual definition gives more intuitive results. On the other hand, at large jet p_T 's

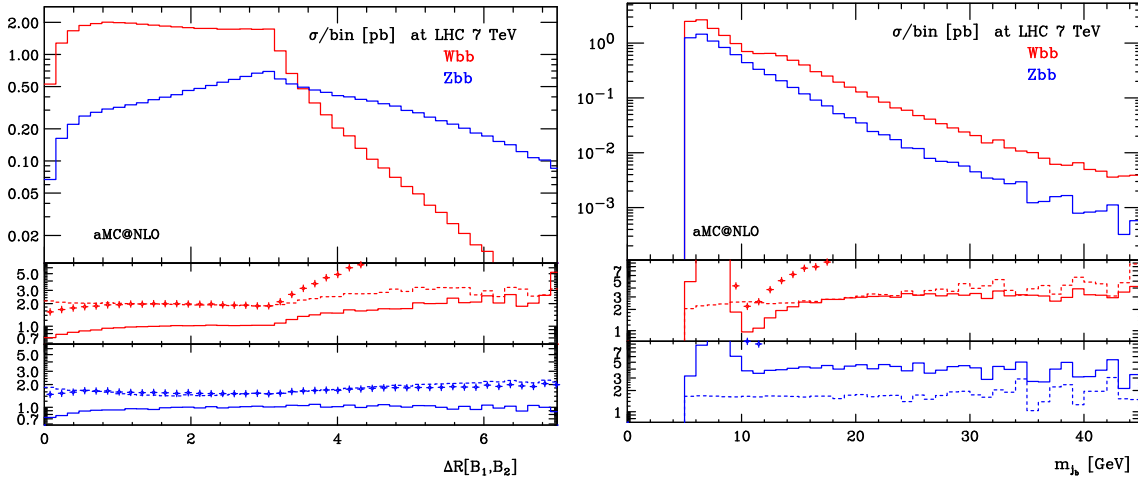


Figure 10: Left panel: ΔR separation between the two hardest b -hadrons (aMC@NLO and aMC@LO) or the b and \bar{b} quarks (NLO and LO) in the event. Right panel: invariant mass of the b -jets, inclusive over all b -jets in the event. The insets follow the same patterns as those in fig. 2.

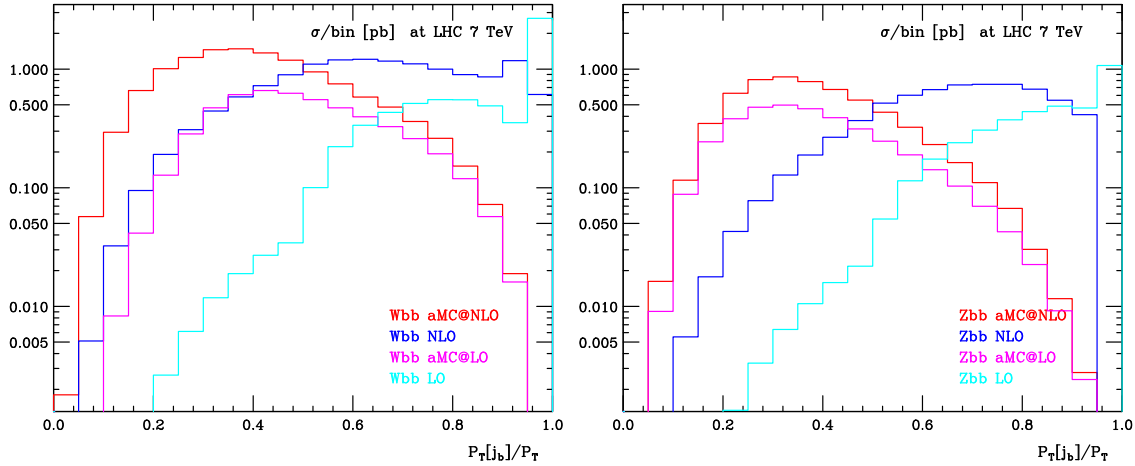


Figure 11: Transverse momentum fraction carried by b -jets. See the text for details.

the onset of the bb -jet contribution to m_{j_b} is largely smeared out.

In fig. 11 we show the ratio of the total transverse momentum $P_T[j_b]$ of b -jets, over the total transverse hadronic momentum P_T ⁵. In the context of parton-level computations, by “hadrons” we simply understand QCD partons. At the parton-level LO, the configurations with one bb -jet or with two b -jets (each of which contains one b quark) give contribution at $P_T[j_b]/P_T = 1$. Configurations with one b -jet that contains only one b quark contribute to $0.5 < P_T[j_b]/P_T < 1$ if the other b quark has $p_T < 20$ GeV (i.e., it is softer than a jet is required to be), while values $P_T[j_b]/P_T < 0.5$ can be obtained when the other b quark has $p_T > 20$ GeV and $|\eta(b)| > 2.5$ (i.e., it is outside the b -jet tagging region in pseudorapidity). What was said above implies that $P_T[j_b]/P_T = 1$ is an infrared-sensitive region, which gives rise to Sudakov logarithms at higher order; this explains the behaviour of the

⁵We stress that P_T is defined without including the underlying event and pile-up contributions.

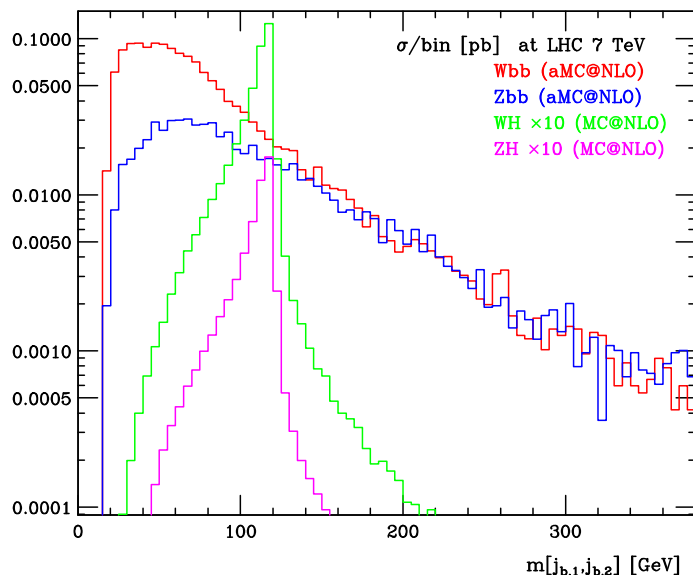


Figure 12: Invariant mass of the pair of the two leading b -jets. $WH(\rightarrow \ell\nu b\bar{b})$, $ZH(\rightarrow \ell^+\ell^-b\bar{b})$, $\ell\nu b\bar{b}$, and $\ell^+\ell^-b\bar{b}$ results are shown, with the former two rescaled by a factor of ten.

parton-level NLO results there. Furthermore, the LO contributions to the $P_T[j_b]/P_T < 0.5$ region decrease when increasing the maximum-pseudorapidity cut on jets. This is only marginally the case at the NLO (because of the presence of a hard light parton in the real-emission contributions), which explains the longer tail of the latter results w.r.t. the LO ones. The arguments above obviously do not apply to the context of an event generator; this is confirmed by the similarity of the aMC@NLO and aMC@LO results. Firstly, at $P_T[j_b]/P_T = 1$ Sudakov logarithms are properly resummed. Secondly, the extra radiation generated by parton showers implies that quite a few hadrons will lie outside b -jets, hence shifting further the $P_T[j_b]/P_T$ results to the left of those relevant to parton-level NLO computations. This shift is also present when passing from the aMC@LO to the aMC@NLO predictions in $Wb\bar{b}$ production, while in the case of $Zb\bar{b}$ production these two results are very similar (up to an overall rescaling by the inclusive K factor). We are finding here the same pattern already discussed for a few observables in this paper. Namely, the opening of gluon-initiated partonic channels at the NLO in $Wb\bar{b}$ production implies a richer hadronic activity w.r.t. the corresponding LO case, which is only marginal in the case of $Zb\bar{b}$ production owing to the dominance of the gg channel already at the LO there. Hence, the relative enhancement of the hadronic activity outside the b -jets when going from aMC@LO to aMC@NLO is stronger for $Wb\bar{b}$ production than is for $Zb\bar{b}$ production.

Finally, as a simple application to Higgs searches of the calculations presented in this paper, we show in fig. 12 the invariant mass of the two leading b -jets in $WH(\rightarrow \ell\nu b\bar{b})$, $ZH(\rightarrow \ell^+\ell^-b\bar{b})$, $\ell\nu b\bar{b}$, and $\ell^+\ell^-b\bar{b}$ events. The former two processes (the “signal”) have been simulated with MC@NLO [32]⁶, with a Higgs mass $m_H = 120$ GeV. The tail at

⁶In the process of validating aMC@NLO, we had checked that it gave results identical to MC@NLO for all the processes implemented in the latter. Hence, we could have equally well employed aMC@NLO to simulate the signal here.

$m[j_{b,1}, j_{b,2}] > m_H$ is due to the fact that the jet momenta are typically larger than those of the b -hadrons they contain, owing to the contributions of other final-state hadrons emerging from initial-state showers. This is compensated by the fact that the b -hadron momenta are only a fraction of those of their parent b quarks, the complementary fraction being lost to radiation which may end up outside the jets. These two effects smear the Higgs peak. Furthermore, in some events the b quarks entering the two hardest b -jets do not arise from the Higgs decay, but from a $g \rightarrow b\bar{b}$ branching in the shower phase. Although rare indeed, these events may result in invariant masses much larger than the Higgs pole mass. The comparison given here is just an example of an analysis in which both the signal and its irreducible backgrounds can be computed at the same precision with (a)MC@NLO, improving upon both fixed-order and LO-based Monte Carlo descriptions.

3. Conclusions and outlook

In this work we have presented results for the $\ell\nu b\bar{b}$ and $\ell^+\ell^-b\bar{b}$ production processes, accurate to the NLO in QCD and that include the matching to parton showers according to the MC@NLO formalism. Our approach is fully general, completely automated, and opens the way to performing comparisons with experimental data from the Tevatron and the LHC at the highest theoretical accuracy attainable nowadays.

By studying a limited but representative set of observables, we have shown that several are the elements to be kept into account in order to achieve reliable and flexible predictions for this class of processes: spin correlations of the final state leptons emerging from the decays of the vector bosons, heavy-quark mass effects, and a realistic description of the final states, obtained thanks to the interface with a shower and hadronisation program. As we have seen, NLO QCD corrections have a highly non-trivial impact, since they lead not only to large enhancements of total rates, but also to significant changes in the shapes of distributions. In this respect, the opening at the NLO of new partonic channels, and in particular of those involving gluons, plays a fundamental role. In general and apart from well-understood cases in which pure perturbative results are not meaningful, one observes that at the NLO level fixed-order and MC-based results are closer to each other than the corresponding LO ones. This is in keeping with naive expectations based on perturbation theory, and it is significant in that it shows that the very large corrections affecting the processes considered here do not pose problems when the matching with parton shower Monte Carlos is carried out according to the MC@NLO method.

Thanks to the aMC@NLO implementation, several QCD issues interesting on their own can now be addressed. One example over all is the study of NLO corrections, mass effects and radiation pattern in final-state gluon splitting, for which $Wb\bar{b}$ production offers a particularly clean environment. Gluon splitting in the initial state and the role of the b PDF (and therefore of different schemes for the predictions of total and differential cross sections) can be assessed by considering $Zb\bar{b}$ production. The outcome of such a study can then be applied to the $Hb\bar{b}$ case. In particular, available predictions in the five-flavour scheme at the NNLO for the fully-inclusive production of a Z in association with bottom quarks [53], and for $Z+1$ b -jet at the NLO [23], can now be compared with our four-flavour-

scheme results. In addition, QCD radiation effects on high- p_T $b\bar{b}$ pairs, which can be merged into one jet, are also of interest in boosted-Higgs searches [54]. Finally, spin correlation effects may also be investigated to gather more insight on the production mechanisms in QCD, and possibly to distinguish them from other competing hard reactions, such as double-parton scatterings. We plan to address some of the above issues in detail in the near future.

We conclude by pointing out that event files relevant to the processes studied in this paper (as well as to others) are publicly available at <http://amcatnlo.cern.ch>. Work to make the use of aMC@NLO public from the same site is in progress.

4. Acknowledgments

S.F. would like to thank Gavin Salam for useful discussions. This research has been supported by the Swiss National Science Foundation (NSF) under contract 200020-126691, by the Belgian IAP Program, BELSPO P6/11-P and the IISN convention 4.4511.10, by the Spanish Ministry of education under contract PR2010-0285, and in part by the US National Science Foundation under grant No. NSF PHY05-51164. F.M. and R.P. thank the financial support of the MEC project FPA2008-02984 (FALCON).

References

- [1] CDF Collaboration, F. Abe *et al.*, *Observation of top quark production in $\bar{p}p$ collisions*, *Phys.Rev.Lett.* **74** (1995) 2626–2631, [[hep-ex/9503002](#)].
- [2] D0 Collaboration, S. Abachi *et al.*, *Observation of the top quark*, *Phys.Rev.Lett.* **74** (1995) 2632–2637, [[hep-ex/9503003](#)].
- [3] D0 Collaboration, V. M. Abazov *et al.*, *Observation of Single Top-Quark Production*, *Phys. Rev. Lett.* **103** (2009) 092001, [[0903.0850](#)].
- [4] CDF Collaboration, T. Aaltonen *et al.*, *First Observation of Electroweak Single Top Quark Production*, *Phys. Rev. Lett.* **103** (2009) 092002, [[0903.0885](#)].
- [5] CDF and D0 Collaboration, T. W. Group, *Combined CDF and D0 upper limits on Standard Model Higgs-boson production with up to 6.7 fb^{-1} of data*, [1007.4587](#).
- [6] CMS Collaboration, G. Bayatian *et al.*, *CMS technical design report, volume II: Physics performance*, *J.Phys.G* **G34** (2007) 995–1579.
- [7] ATLAS Collaboration, G. Aad *et al.*, *Expected performance of the ATLAS experiment - detector, trigger and physics*, [0901.0512](#).
- [8] P. B. Arnold and M. H. Reno, *The complete computation of high- p_t W and Z production in 2nd order QCD*, *Nucl. Phys.* **B319** (1989) 37.
- [9] J. M. Campbell and R. K. Ellis, *Next-to-leading order corrections to W+2 jet and Z+2 jet production at hadron colliders*, *Phys. Rev.* **D65** (2002) 113007, [[hep-ph/0202176](#)].
- [10] C. F. Berger *et al.*, *Next-to-leading order QCD predictions for W+3-jet distributions at hadron colliders*, *Phys. Rev.* **D80** (2009) 074036, [[0907.1984](#)].

- [11] C. F. Berger *et al.*, *Precise predictions for $W+3$ jet production at hadron colliders*, *Phys. Rev. Lett.* **102** (2009) 222001, [0902.2760].
- [12] K. Melnikov and G. Zanderighi, *$W+3$ jet production at the LHC as a signal or background*, *Phys. Rev.* **D81** (2010) 074025, [0910.3671].
- [13] C. F. Berger *et al.*, *Precise predictions for $W+4$ jet production at the Large Hadron Collider*, *Phys. Rev. Lett.* **106** (2011) 092001, [1009.2338].
- [14] R. K. Ellis, G. Martinelli, and R. Petronzio, *Lepton Pair Production at Large Transverse Momentum in Second Order QCD*, *Nucl. Phys.* **B211** (1983) 106.
- [15] C. F. Berger *et al.*, *Next-to-leading order QCD predictions for Z/γ^*+3 -jet distributions at the Tevatron*, *Phys. Rev.* **D82** (2010) 074002, [1004.1659].
- [16] R. Ellis and S. Veseli, *Strong radiative corrections to $Wb\bar{b}$ production in $p\bar{p}$ collisions*, *Phys.Rev.* **D60** (1999) 011501, [hep-ph/9810489].
- [17] J. M. Campbell and R. K. Ellis, *Radiative corrections to $Zb\bar{b}$ production*, *Phys. Rev.* **D62** (2000) 114012, [hep-ph/0006304].
- [18] F. FebresCordero, L. Reina, and D. Wackerroth, *NLO QCD corrections to W boson production with a massive b -quark jet pair at the Tevatron $p\bar{p}$ collider*, *Phys.Rev.* **D74** (2006) 034007, [hep-ph/0606102].
- [19] F. Febres Cordero, L. Reina, and D. Wackerroth, *NLO QCD corrections to $Zb\bar{b}$ production with massive bottom quarks at the Fermilab Tevatron*, *Phys.Rev.* **D78** (2008) 074014, [0806.0808].
- [20] F. Febres Cordero, L. Reina, and D. Wackerroth, *W - and Z -boson production with a massive bottom-quark pair at the Large Hadron Collider*, *Phys.Rev.* **D80** (2009) 034015, [0906.1923].
- [21] S. Badger, J. M. Campbell, and R. K. Ellis, *QCD corrections to the hadronic production of a heavy quark pair and a W -boson including decay correlations*, *JHEP* **03** (2011) 027, [1011.6647].
- [22] J. M. Campbell *et al.*, *Associated production of a W boson and one b jet*, *Phys. Rev.* **D79** (2009) 034023, [0809.3003].
- [23] J. M. Campbell, R. K. Ellis, F. Maltoni, and S. Willenbrock, *Associated production of a Z Boson and a single heavy quark jet*, *Phys. Rev.* **D69** (2004) 074021, [hep-ph/0312024].
- [24] J. M. Campbell, R. K. Ellis, F. Maltoni, and S. Willenbrock, *Production of a W boson and two jets with one b -quark tag*, *Phys. Rev.* **D75** (2007) 054015, [hep-ph/0611348].
- [25] J. M. Campbell, R. K. Ellis, F. Maltoni, and S. Willenbrock, *Production of a Z boson and two jets with one heavy-quark tag*, *Phys. Rev.* **D73** (2006) 054007, [hep-ph/0510362].
- [26] **CDF** Collaboration, D. Acosta *et al.*, *Study of the heavy flavor content of jets produced in association with W bosons in $p\bar{p}$ collisions at $\sqrt{s} = 1.8$ TeV*, *Phys.Rev.* **D65** (2002) 052007, [hep-ex/0109012].
- [27] **CDF** Collaboration, T. Aaltonen *et al.*, *Measurement of cross sections for b -jet production in events with a Z boson in $p\bar{p}$ collisions at $\sqrt{s} = 1.96$ TeV*, *Phys. Rev.* **D79** (2009) 052008, [0812.4458].
- [28] **CDF** Collaboration, T. Aaltonen *et al.*, *First measurement of the b -jet cross section in events with a W boson in $p\bar{p}$ collisions at $\sqrt{s} = 1.96$ TeV*, *Phys.Rev.Lett.* **104** (2010) 131801, [0909.1505].

- [29] **D0** Collaboration, V. M. Abazov *et al.*, *A measurement of the ratio of inclusive cross sections $\sigma(p\bar{p} \rightarrow Z + b \text{ jet})/\sigma(p\bar{p} \rightarrow Z + \text{jet})$ at $\sqrt{s} = 1.96 \text{ TeV}$* , *Phys.Rev.* **D83** (2011) 031105, [1010.6203].
- [30] **CMS** Collaboration, V. Ciulli *et al.*, *W/Z+jets results from CMS*, *CMS CR-2011/073* (2011).
- [31] **ATLAS** Collaboration, *Measurement of the production cross section for W-bosons in association with jets in collisions using 33 pb^{-1} at $\sqrt{s} = 7 \text{ TeV}$ with the ATLAS detector*, *ATLAS-CONF-2011-060* (2011).
- [32] S. Frixione and B. R. Webber, *Matching NLO QCD computations and parton shower simulations*, *JHEP* **06** (2002) 029, [hep-ph/0204244].
- [33] R. Frederix, S. Frixione, V. Hirschi, F. Maltoni, R. Pittau, and P. Torrielli, *Scalar and pseudoscalar Higgs production in association with a top-antitop pair*, 1104.5613.
- [34] V. Hirschi, R. Frederix, S. Frixione, M. V. Garzelli, F. Maltoni, and R. Pittau, *Automation of one-loop QCD corrections*, *JHEP* **05** (2011) 044, [1103.0621].
- [35] G. Ossola, C. G. Papadopoulos, and R. Pittau, *Reducing full one-loop amplitudes to scalar integrals at the integrand level*, *Nucl.Phys.* **B763** (2007) 147–169, [hep-ph/0609007].
- [36] G. Ossola, C. G. Papadopoulos, and R. Pittau, *CutTools: a program implementing the OPP reduction method to compute one-loop amplitudes*, *JHEP* **03** (2008) 042, [0711.3596].
- [37] S. Frixione, Z. Kunszt, and A. Signer, *Three jet cross-sections to next-to-leading order*, *Nucl. Phys.* **B467** (1996) 399–442, [hep-ph/9512328].
- [38] R. Frederix, S. Frixione, F. Maltoni, and T. Stelzer, *Automation of next-to-leading order computations in QCD: the FKS subtraction*, *JHEP* **10** (2009) 003, [0908.4272].
- [39] C. Oleari and L. Reina, *Wb \bar{b} production in POWHEG*, 1105.4488.
- [40] S. Alioli, P. Nason, C. Oleari, and E. Re, *A general framework for implementing NLO calculations in shower Monte Carlo programs: the POWHEG BOX*, *JHEP* **06** (2010) 043, [1002.2581].
- [41] A. D. Martin, W. J. Stirling, R. S. Thorne, and G. Watt, *Parton distributions for the LHC*, *Eur. Phys. J.* **C63** (2009) 189–285, [0901.0002].
- [42] G. Marchesini *et al.*, *HERWIG: A Monte Carlo event generator for simulating hadron emission reactions with interfering gluons. Version 5.1 - April 1991*, *Comput. Phys. Commun.* **67** (1992) 465–508.
- [43] G. Corcella *et al.*, *HERWIG 6.5: an event generator for Hadron Emission Reactions With Interfering Gluons (including supersymmetric processes)*, *JHEP* **01** (2001) 010, [hep-ph/0011363].
- [44] G. Corcella *et al.*, *HERWIG 6.5 release note*, hep-ph/0210213.
- [45] M. Bahr *et al.*, *Herwig++ Physics and Manual*, *Eur. Phys. J.* **C58** (2008) 639–707, [0803.0883].
- [46] T. Sjostrand, S. Mrenna, and P. Z. Skands, *PYTHIA 6.4 Physics and Manual*, *JHEP* **05** (2006) 026, [hep-ph/0603175].
- [47] S. Frixione, F. Stoeckli, P. Torrielli, and B. R. Webber, *NLO QCD corrections in Herwig++ with MC@NLO*, *JHEP* **01** (2011) 053, [1010.0568].

- [48] P. Torrielli and S. Frixione, *Matching NLO QCD computations with PYTHIA using MC@NLO*, *JHEP* **04** (2010) 110, [[1002.4293](#)].
- [49] M. Cacciari, G. P. Salam, and G. Soyez, *The anti- k_t jet clustering algorithm*, *JHEP* **04** (2008) 063, [[0802.1189](#)].
- [50] A. Banfi, G. P. Salam, and G. Zanderighi, *Infrared safe definition of jet flavor*, *Eur. Phys. J.* **C47** (2006) 113–124, [[hep-ph/0601139](#)].
- [51] J. Alwall *et al.*, *MadGraph/MadEvent v4: the new web generation*, *JHEP* **09** (2007) 028, [[0706.2334](#)].
- [52] Z. Bern *et al.*, *Left-Handed W Bosons at the LHC*, *Phys. Rev.* **D84** (2011) 034008, [[1103.5445](#)].
- [53] F. Maltoni, T. McElmurry, and S. Willenbrock, *Inclusive production of a Higgs or Z boson in association with heavy quarks*, *Phys.Rev.* **D72** (2005) 074024, [[hep-ph/0505014](#)].
- [54] J. M. Butterworth, A. R. Davison, M. Rubin, and G. P. Salam, *Jet substructure as a new Higgs search channel at the LHC*, *Phys. Rev. Lett.* **100** (2008) 242001, [[0802.2470](#)].